

Pressure Tuning of the Optical Properties of GaAs Nanowires

Ilaria Zardo,^{†,*,#,*} Sara Yazji,[†] Carlo Marini,^{§,||} Emanuele Uccelli,^{†,||,△} Anna Fontcuberta i Morral,^{||} Gerhard Abstreiter,^{†,*} and Paolo Postorino[§]

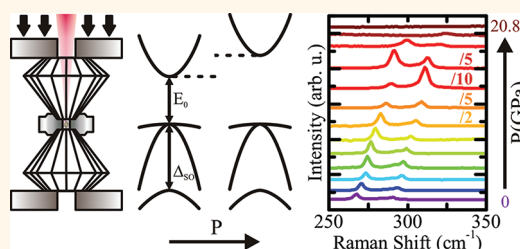
[†]Walter Schottky Institut and Physik Department, Technische Universität München, Am Coulombwall 4, D-85748 Garching, Germany, [‡]Institute for Advanced Study, Technische Universität München, Lichtenbergstrasse 2a, D-85748 Garching, Germany, [§]IOM-CNR and Dipartimento di Fisica, Università di Roma Sapienza, P.le Aldo Moro 5, I-00185 Roma, Italy, ^{||}European Synchrotron Radiation Facility, 6 Rue Jules Horowitz, BP 220, F-38043 Grenoble Cedex, France, and ^{||}Laboratoire des Matériaux Semiconducteurs, Institut des Matériaux, Ecole Polytechnique Fédérale de Lausanne, CH-1015 Lausanne, Switzerland. [#]Present address: Applied Physics, Photonics & Semiconductor Nanophysics, Eindhoven University of Technology, 5600 MB Eindhoven, The Netherlands. [△]Present address: IBM Research—Zurich, 8803 Rüschlikon, Switzerland.

Semiconductors with dimensions on the nanometer scale can nowadays be synthesized under highly controlled conditions by several techniques. Their size, geometry, peculiar lattice structure, which often depends on the growth conditions, and the high surface-to-volume ratio can induce mechanical, electronic, and optical properties remarkably different from those of the bulk counterparts.^{1–3}

Optical spectroscopy techniques, such as Raman and photoluminescence (PL), have been extensively and successfully applied to achieve a deep understanding of the physical properties of bulk semiconductors. Moreover, starting from the 1970s, spectroscopic investigations took full advantage of high-pressure techniques, and the peculiar pressure dependence of electronic and structural properties of many diamond and zincblende semiconductors was systematically investigated.⁴ These systems show pressure-induced structural transitions as well as a strong pressure dependence of the band gaps. It is worth noticing that pressure tuning of the band gaps, besides photoluminescence, affects also the Raman response, since the scattering process is mediated by electrons *via* electron–hole pair formation and recombination. Considering that the electronic states enter in the Raman scattering cross section, resonant Raman scattering provides information on the electronic states and electron–phonon and phonon–phonon interactions.

In the last years, spectroscopic investigations have been extended also to nanostructured semiconductors and quite recently to the study of the pressure dependence of their physical properties. Semiconductor nanowires have, in particular, stimulated

ABSTRACT



The tuning of the optical and electronic properties of semiconductor nanowires can be achieved by crystal phase engineering. Zinc-blende and diamond semiconductors exhibit pressure-induced structural transitions as well as a strong pressure dependence of the band gaps. When reduced to nanoscale dimensions, new phenomena may appear. We demonstrate the tuning of the optical properties of GaAs nanowires and the induction of a phase transition by applying an external pressure. The dependence of the E_0 gap on the applied pressure was measured, and a direct-to-indirect transition was found. Resonant Raman scattering was obtained by pressure tuning of the E_0 and the $E_0 + \Delta_{s0}$ gaps with respect to the excitation energy. The resonances of the longitudinal optical modes LO and 2LO indicate the presence of electron–phonon Fröhlich interactions. These measurements show for the first time a variation of ionicity in GaAs when in nanowire form. Furthermore, the dependence of the lattice constant on applied pressure was estimated. Finally, we found a clear indication of a structural transition above 16 GPa.

KEYWORDS: nanowires · optical properties · high pressure · Raman spectroscopy · resonant Raman

extensive investigations because of the wide range of potential technological applications ranging from electronic devices to sensors and to energy conversion. In this respect, Raman and resonant Raman spectroscopy have proven to be powerful tools.^{5–8} Since functional properties of nanowires depend on both their structural properties and electronic band gaps, a

* Address correspondence to ilaria.zardo@wsi.tum.de.

Received for review January 16, 2012 and accepted March 24, 2012.

Published online March 24, 2012
10.1021/nn300228u

© 2012 American Chemical Society

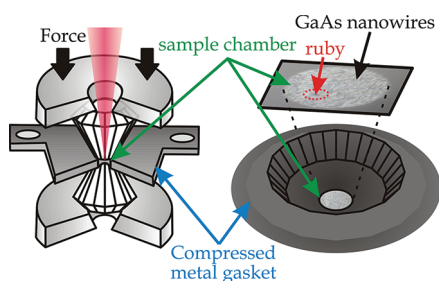


Figure 1. Schematic of the diamond anvil cell.

high-pressure spectroscopic study can provide valuable information.⁹

In this paper we focus on the pressure response of GaAs nanowires measured by photoluminescence and Raman spectroscopy techniques at room temperature. The availability of a wide set of spectroscopic data collected in the past on bulk GaAs under ambient and high-pressure conditions, and recently on ambient-pressure nanowires, enabled a careful nanowire/bulk comparison.

RESULTS AND DISCUSSION

Direct-to-Indirect Transition. Light scattering and photoluminescence experiments on zinc-blende GaAs nanowires under hydrostatic pressure up to 20.8 GPa were performed by using a diamond anvil cell (DAC), shown in Figure 1 and described in detail in the Methods section. As mentioned above, diamond and zinc-blende semiconductors exhibit a peculiar, strong pressure-dependence of the band gaps with pressure coefficients, typically on the order of 10 meV/kbar,¹⁰ which can remarkably depend on the different energy band extrema.^{10,11} A scheme of the ambient-pressure band structure of bulk GaAs around the Γ -point is shown in Figure 2a. It has been found that, under compression, the E_0 energy gap exhibits a strong shift, nonlinearly dependent on the applied pressure.^{12,13} In our experiments, the PL signal of nanowire ensembles was measured first at ambient pressure (Figure 2b). The PL peak was found at about 1.43 eV, with a relatively low intensity. The energy position corresponds to the E_0 energy gap of GaAs at room temperature. A relatively low PL intensity is expected at room temperature for uncoated nanowires used for these experiments since nonradiative recombination occurs due to the presence of surface states.¹⁴ The observed abrupt and strong increase of the PL intensity after closing the DAC (see Figure 2b) can be possibly ascribed to the passivation of the surface states after embedding the nanowires in the hydrostatic medium, especially considering that the nanowire density typically decreases upon closing the DAC. On applying pressure up to ~ 5 GPa, the position of the PL peak shifts toward higher energies (lower values of Raman shift) as shown in Figure 2b. At pressures higher than 5 GPa, the PL signal moved out of the Stokes spectral range, which means

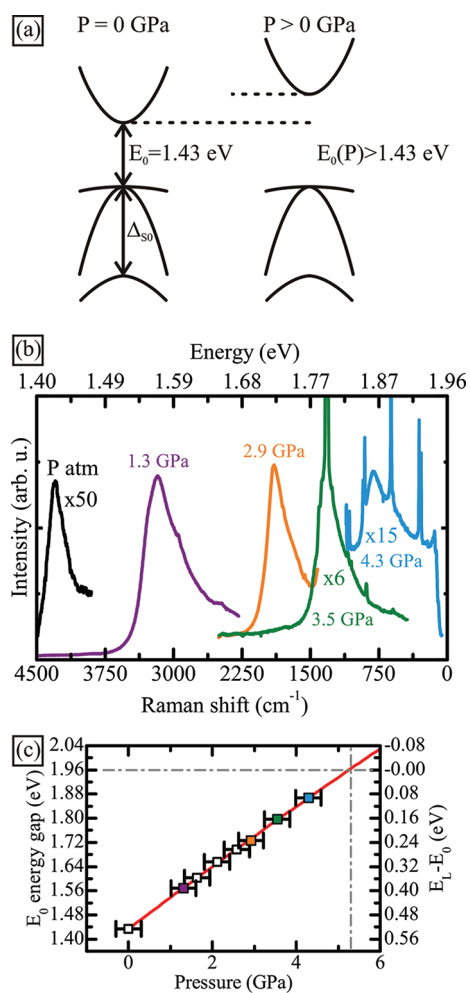


Figure 2. (a) Schematic band diagram for zinc-blende GaAs near the Brillouin zone center at ambient pressure (left) and at high pressure (right). (b) Selected PL spectra collected at different pressures. The spectrum at ambient pressure, as well as those at higher pressures, has been multiplied by a constant factor. The spectrum at ambient pressure was collected before loading the hydrostatic medium and closing the cell (see text). (c) Energy of the PL emission (left-hand scale) as a function of the applied pressure. Filled squares correspond to the spectra plotted in (b). Solid line is a polynomial fit to the data. Dashed gray lines indicate the resonance between E_L and E_0 at 5.3 GPa. The right-hand scale provides the energy difference between the laser energy ($E_L = 1.959$ eV) and the pressure-dependent direct band gap energy E_0 .

to higher energies than the laser excitation energy ($E_L = 1.959$ eV). The sharp peaks in the PL spectra are ascribed to first and higher order Raman spectra of the GaAs nanowires, enhanced due to resonance conditions (see next section).

Although a rigorous quantitative analysis of the PL peak intensities as a function of the pressure cannot be given, since the energy dependence of the CCD efficiency is not flat over the whole energy range, qualitative considerations can be drawn. After the initial increase on closing the cell the progressive decrease of the PL intensity with pressure is rather obvious (notice the multiplicative factors given in Figure 2b).

This behavior is in agreement with the increase of the energy gap and the band gap transition from direct to indirect under pressure.^{13,15}

In Figure 2c, the energetic position of the PL emission is plotted as a function of the applied pressure up to 5 GPa. According to previous studies,^{12,13} the dependence of the E_0 gap on the pressure was fitted with the polynomial function

$$E_0(\text{eV}) = 1.43 + 1.05 \times 10^{-1}P - 8.84 \times 10^{-4}P^2 \quad (1)$$

with P in GPa. Looking at the value of the second-order coefficient, it is clear that over the present low-pressure range the linear part is dominant. Due to the pressure dependence, schematized in Figure 2a, the band gap enters into resonance with the excitation energy ($E_L = 1.959$ eV), providing resonant conditions for the Raman scattering. The energy difference $E_L - E_0$ between laser energy and direct band gap energy was extrapolated from the polynomial fit, and it is given in Figure 2c as the right-hand scale. Assuming a constant spin–orbit splitting of $\Delta_{SO} = 0.34$ eV on volume compression (see schematic in Figure 2a), the pressure dependence of the energy difference $E_L - (E_0 + \Delta_{SO})$ can be estimated from eq 1. The E_0 and the $E_0 + \Delta_{SO}$ energy gaps are in resonance with the excitation energy at 5.3 and 1.8 GPa, respectively.

Tuning of Band Gaps and Fröhlich Interaction. High-pressure Raman spectra of GaAs nanowires, collected on a nanowire ensemble, are plotted in Figure 3. For the sake of clarity, selected spectra up to 20.8 GPa have been shifted vertically. For $P > 16$ GPa, no distinguishable feature was observed in the Raman spectra. From ambient pressure up to 16 GPa, Raman spectra are characterized, on the low-frequency side, by peaks ascribed to transversal optical (TO), surface optical (SO), and longitudinal optical (LO) modes. In addition, peaks of higher order modes appear on the high-frequency side at certain pressures. All phonon peaks shift toward higher frequencies with applied pressure, and their intensities strongly vary with pressure.

The intensities of the TO, LO, and 2LO modes were normalized to the intensity of the methanol–ethanol (EM) peak at 900 cm^{-1} , which is more or less independent of the applied pressure (not shown here). In Figure 4, the modes are plotted as a function of pressure (linear, bottom scale) and of the energy difference $E_L - E_0$ (upper scale). Since the Raman intensity depends on the density of the nanowires, which is different in the two series of measurements (see Methods section), the low pressure series (LPS) data have been normalized to the high pressure series (HPS) data by adjusting the measurements of both series at 2.1 GPa for matching the resonance profiles. The resonant behavior of Raman scattering by TO and LO phonons near the E_0 gap appears clearly at ~ 5 GPa. Another less pronounced peak centered between

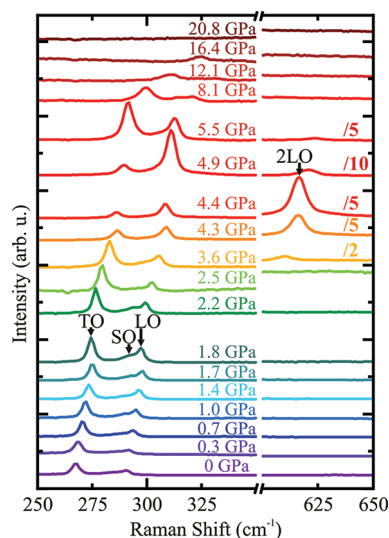


Figure 3. Pressure dependence of the Raman spectra from 0 to 20.8 GPa. For clarity, only selected pressures are plotted and have been shifted vertically. Furthermore, the spectra collected between 3 and 8 GPa have been scaled down by the factors given in the figure. The TO, SO, LO, and 2LO are labeled and indicated by arrows in two selected spectra.

1.4 and 1.8 GPa can be attributed to the resonance near the $E_0 + \Delta_{SO}$ gap. The high-intensity tail at low pressure contains also the contribution of the outgoing resonant scattering processes. Indeed, the outgoing resonances (E_0 and $E_0 + \Delta_{SO} \approx \hbar\omega_s$) occur at lower pressure than the incoming resonance (E_0 and $E_0 + \Delta_{SO} \approx \hbar\omega_i$). Interestingly, under resonance conditions, the intensity of the LO mode gains more or less 2 orders of magnitude, while that of the TO mode only about 1 order of magnitude. The ambient-pressure studies on zinc-blende GaAs nanowires proved that the LO mode is forbidden in backscattering from the nanowire facets, as expected from the Raman selection rules.⁵ In the present experiment, therefore, the strong E_0 resonance of the forbidden LO mode is an indication of the electron–phonon Fröhlich interaction.^{7,16} The Fröhlich interaction is confirmed by the resonant behavior of the 2LO mode, shown also in Figure 4. The resonance of the 2LO mode occurs at 4.4 GPa, the pressure at which the E_0 energy gap is about 1.87 eV. Therefore, the resonance of the 2LO occurs at $E_0 + 2\hbar\omega(\text{LO})$. In other words, this is a sharp outgoing resonance. It is worth noticing here that this can be seen even from the energy separation between the two resonance peaks. While in the resonance profile of the LO mode the energy separation of the two peaks is $\Delta E \approx 0.35$ eV, close to $\Delta_{SO} \approx 0.34$ eV, in the resonance profile of the 2LO mode the energy separation of the two peaks is $\Delta E \approx 0.30$ eV, due to the sharp outgoing resonance at the E_0 gap. The intensity ratio $I(2\text{LO})/I(\text{LO})$ at $E_0 + 2\hbar\omega(\text{LO})$ is 4.4, confirming that the Fröhlich coupling is stronger in GaAs nanowires than in the bulk, as already observed in resonant Raman scattering experiments on a single GaAs nanowire.⁷ In our case,

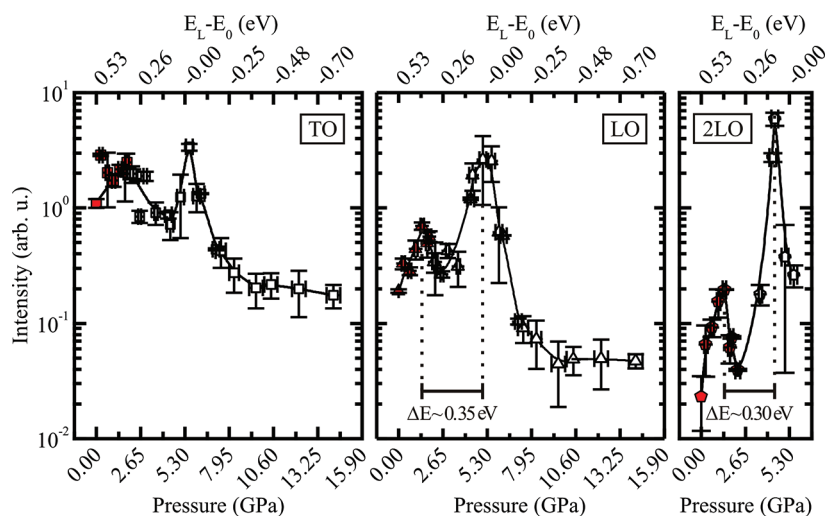


Figure 4. Pressure induced E_0 and $E_0 + \Delta_{SO}$ resonances of the TO (squares), LO (triangles), and 2LO (pentagons) modes in GaAs nanowires. Filled and open symbols correspond to the LP and HP series, respectively. The intensities, normalized to the intensity of the EM peak, are shown versus pressure (linear bottom scale) and versus the energy difference $E_L - E_0$ (top scale). Solid lines are guide to the eye.

we can exclude coupling with charged surface states, which are passivated by the hydrostatic medium. Our results suggest an enhancement of the electron–phonon interaction probably due to confinement. Indeed, the nanowires measured in this work have a diameter of about 80 nm, for which a small confinement can be expected. Interestingly, the intensity of the weak SO phonon mode does not show a clear dependence on applied pressure. This could indicate that the pressure does not induce any significant discontinuous change in the morphology of the nanowires.

Lattice Response to Pressure: Covalence/Ionicity of the Bonds. The measured frequencies of the TO, SO, and LO modes are displayed in Figure 5 as a function of the applied pressure (top scale) and of the relative lattice compression $-(\Delta a)/(a_0)$ (linear, bottom scale). The latter has been obtained exploiting Murnaghan's equation:¹⁷

$$P = \frac{B_0}{B'_0} \left[\left(\frac{a_0}{a} \right)^{3B'_0} - 1 \right] \quad (2)$$

where $B_0 = -V((\partial P)/(\partial V))$ is the isothermal bulk modulus, with V the volume of the unit cell and B'_0 its derivative with respect to the pressure. To the best of our knowledge, the bulk modulus and the derivative have not been measured yet on GaAs nanowires; therefore we used the values of $B_0 = 74.66$ GPa and $B'_0 = 4.67$, reported for bulk GaAs.¹⁸ It is worth noting here that, although the bulk modulus is expected to increase with decreasing nanostructure size,^{19,20} no big variation was found experimentally²¹ or predicted²² for semiconductor nanowires with diameter comparable to those of this study, *i.e.*, about 80 nm.

In Figure 5, the solid (dashed) lines are polynomial (linear) fits to the data, which show the following dependence of the optical phonon frequencies on

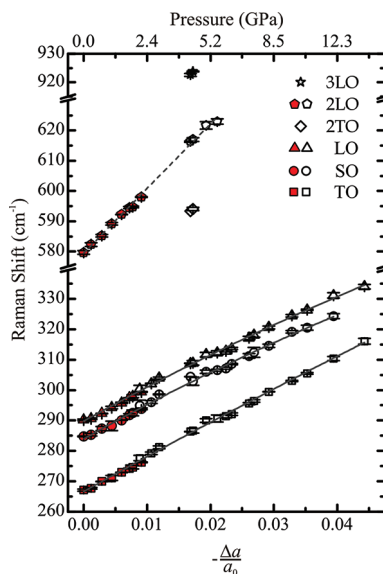


Figure 5. Raman shift of the optical modes as a function of lattice constant (linear, bottom scale) and of applied pressure (nonlinear top scale). Filled and open symbols correspond to the LP and HP series, respectively. Solid (dashed) lines are polynomial (linear) fits to the data.

relative lattice compression:

$$\begin{aligned} \omega_{\text{TO}} &= (266.7 \pm 0.4) + (1.16 \pm 0.04) \times 10^3 (-\Delta a/a_0) \\ &\quad - (1.3 \pm 0.9) \times 10^3 (-\Delta a/a_0)^2 \\ \omega_{\text{SO}} &= (284.8 \pm 0.3) + (1.02 \pm 0.01) \times 10^3 (-\Delta a/a_0) \\ &\quad - (3.7 \pm 1.1) \times 10^3 (-\Delta a/a_0)^2 \\ \omega_{\text{LO}} &= (289.8 \pm 0.4) + (1.15 \pm 0.04) \times 10^3 (-\Delta a/a_0) \\ &\quad - (3.2 \pm 0.9) \times 10^3 (-\Delta a/a_0)^2 \\ \omega_{\text{2LO}} &= (579.5 \pm 0.5) + (2.13 \pm 0.03) \times 10^3 (-\Delta a/a_0) \end{aligned} \quad (3)$$

where the frequencies ω are in cm^{-1} . The TO, SO, and LO modes show a slightly sublinear dependence

on $-\Delta a/a_0$, while the 2LO mode is described better by a linear dependence on $-\Delta a/a_0$. Although the values obtained from the fitting procedure are quite comparable within the statistical error with those obtained in the bulk, the coefficient of the quadratic term of the TO mode slightly deviates.²³ Furthermore, the mean value of the coefficient of the quadratic term for the TO and LO modes deviates in the opposite direction.

The dependence of the optical phonons on the pressure is also sublinear and given by

$$\begin{aligned}\omega_{\text{TO}} &= (267.2 \pm 0.4) + (4.70 \pm 0.14)P - (0.09 \pm 0.01)P^2 \\ \omega_{\text{SO}} &= (284.5 \pm 0.3) + (4.65 \pm 0.15)P - (0.11 \pm 0.15)P^2 \\ \omega_{\text{LO}} &= (290.4 \pm 0.4) + (4.56 \pm 0.13)P - (0.10 \pm 0.01)P^2 \\ \omega_{\text{2LO}} &= (579.4 \pm 0.6) + (9.8 \pm 0.7)P - (0.30 \pm 0.12)P^2\end{aligned}\quad (4)$$

where the frequencies ω are in cm^{-1} and P is in GPa. The sublinear dependences on P are usually observed for the optical phonons of diamond and zinc-blende structures,⁴ although in the low-pressure range the pressure dependence of the modes can be approximated by a linear function of P .^{4,24} The pressure-induced phonon frequency shift is usually discussed in terms of the Grüneisen parameter, which describes the shift in frequency of a phonon due to a variation of the lattice's volume as a result of temperature or pressure change and is given by²⁵

$$\gamma = \frac{\partial \ln \omega}{\partial \ln V} = \left(\frac{B_0}{\omega_0} \right) \left(\frac{\partial \omega}{\partial P} \right)_{P=0} \quad (5)$$

Typical values of γ for optical phonons of diamond and zinc-blende structures are in the range between +1.0 and +2.5.^{4,25} For the nanowires we obtain the following values:

$$\begin{aligned}\gamma_{\text{TO}} &= 1.31 \pm 0.04 \\ \gamma_{\text{SO}} &= 1.22 \pm 0.04 \\ \gamma_{\text{LO}} &= 1.17 \pm 0.03 \\ \gamma_{\text{2LO}} &= 1.26 \pm 0.09\end{aligned}\quad (6)$$

These values are slightly different from those obtained in bulk GaAs, where $\gamma_{\text{TO}} \approx 1.39$ and $\gamma_{\text{LO}} \approx 1.23$ at the Γ point,²⁵ for exactly the same pressure range. Values close to 1 are expected for the covalent materials.²⁵ Instead, higher values are expected in the case of ionic zinc-blende materials, especially for the TO mode. The Grüneisen parameters found in the present work for the TO(Γ) and LO(Γ) modes are reduced by about 6% with respect to the bulk values. This variation is with respect to values obtained by Trommer *et al.*²⁶ in the same pressure range and using the same fitting function. For comparison, we also calculated the values of the Grüneisen parameters with a linear fit up to 7 GPa. In this case, we obtain $\gamma_{\text{TO}} = 1.14 \pm 0.03$ and $\gamma_{\text{LO}} = 0.97 \pm 0.03$, while it was $\gamma_{\text{TO}} = 1.22 \pm 0.03$ and $\gamma_{\text{LO}} = 1.14 \pm 0.03$ for the bulk,²⁶ and the variation with respect to the bulk is even as high as 15% for γ_{LO} . The reduction of these parameters can be

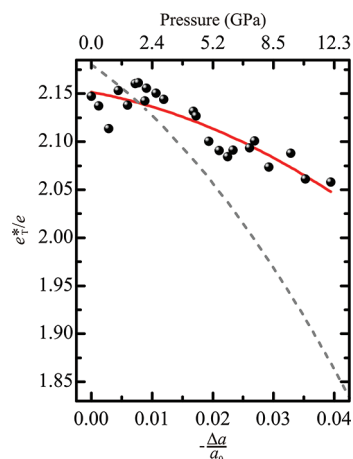


Figure 6. Born's transverse dynamic effective charge as a function of lattice constant (linear, lower scale) and of applied pressure (nonlinear, upper scale). Solid line is the polynomial fit to the data; dashed line is the polynomial fit curve from bulk GaAs, according to ref 26.

understood as a smaller variation of the phonon frequency due to a variation of the volume of the unit cell. The reason for this pressure response is still unclear, but the one-dimensional nature of the system could play a role, although the influence of low-density twin defects cannot be completely excluded. Moreover, it is interesting to note that the γ_{2LO} is comparable in the error with γ_{LO} ; that is, the frequency shift of the 2LO(ω) with pressure is approximately double that of the LO(ω). Weinstein and coauthors found a different shift with pressure of the two modes in GaP.²⁷ Trommer and coauthors suggested that the reason for this lies in a different degree of resonance due to the pressure tuning of the band gap.²³ Our results point in a different direction, or suggest that the dimensionality of the system affects the degree of resonance.

While the SO–LO splitting is approximately constant, the LO–TO splitting decreases with increasing pressure, as observed in most of the zinc-blende-type materials.²³ We found a linear dependence of the TO–LO splitting on the pressure. The frequency difference $\omega_{\text{LO}}^2 - \omega_{\text{TO}}^2$ is given by²⁵

$$\omega_{\text{LO}}^2 - \omega_{\text{TO}}^2 = \frac{4\pi(e^*_{\text{T}})^2}{\varepsilon_{\infty}\mu V} = \omega_{\text{TO}}^2 \frac{\varepsilon_0 - \varepsilon_{\infty}}{\varepsilon_{\infty}} \quad (7)$$

with μ being the reduced mass, V the volume of the primitive cell, and ε_{∞} the infrared dielectric constant (in atomic units). Equation 7 defines Born's transverse dynamic effective charge e^*_{T} , which can be seen as a measure of the ionicity of a compound. The dependence of e^*_{T} on the lattice constant is plotted in Figure 6, assuming that $d \ln(\varepsilon_{\infty}) = 3d \ln a$ as for bulk GaAs.²³ The data can be fitted with a polynomial form:

$$e^*_{\text{T}} = 2.15 - 1.1 \left(-\frac{\Delta a}{a_0} \right) - 38 \left(-\frac{\Delta a}{a_0} \right)^2 \quad (8)$$

The pressure-induced reduction of the dynamic effective charge indicates that the system becomes more covalent upon compression. A similar behavior has been found for e^*_T in bulk material although with a different pressure dependence,^{23,28} indicating a different dependence of the ionic character of the system on lattice constant. Indeed, in the case of nanowires, the “ionicity” of the system is reduced at ambient pressure with respect to the bulk, in agreement with the reduction of the Grüneisen parameters. Then, upon compression, the nanowire system is more resistant to an increase of the covalency than the bulk.

The Grüneisen parameter γ_{e^*} for Born's dynamic charge is defined as

$$\begin{aligned} \gamma_{e^*} &= \frac{d \ln e^*}{d \ln V} \\ &= \frac{1}{2} + \frac{1}{2} \gamma_{\epsilon_\infty} + \gamma_{LO} + (\gamma_{LO} - \gamma_{TO}) \frac{\epsilon_\infty}{\epsilon_0 - \epsilon_\infty} \quad (9) \end{aligned}$$

Assuming $\gamma_{\epsilon_\infty} = 1.0$ ¹⁶ and using the obtained values of the Grüneisen parameter, we get $\gamma_{e^*} = -0.56 \pm 0.32$, where the relatively large error is mainly determined by the uncertainty in $\gamma_{LO/TO}$. We notice that the negative value is determined by the pressure-induced reduction of e^*_T , in agreement with most of the zinc-blende semiconductors. However, also this value is slightly different from what was obtained in bulk GaAs.²⁵ This is again related to the anomalous Grüneisen parameters for the TO and the LO modes. Further investigation is needed in order to gain a better understanding of this anomaly.

The linewidths of the Raman phonon peaks are related to the anharmonic coupling of two phonons and to isotope mass fluctuations.⁴ Therefore, the dependence of the phonon linewidths on pressure can provide information on phonon–phonon interaction and/or isotope disorder. The fwhm of the TO and LO modes of the GaAs nanowires are plotted in Figure 7 as a function of pressure. A clear dependence of the fwhm on pressure can be observed, although crystal defects may contribute to the initial broadening of the peaks, as does a distribution in the position of the Raman peaks due to the fact that the measurements are realized on ensembles of nanowires. The fwhm of the LO mode is approximately constant, with a pressure up to 10–12 GPa. The apparent increase of the fwhm of the LO mode for $P \geq 12$ GPa is simultaneous to a huge increase of the relative error bars due to the impossibility to unambiguously distinguish the LO and SO peaks. Therefore, we can assume, as far as the fwhm values are reliably determined, that the width of the LO is weakly affected by pressure, as already observed in bulk GaP.²⁹ Differently, the fwhm of the TO mode slightly decreases up to $P \approx 2$ GPa and then is increasing linearly for $P > 2$ GPa, indicating the relevance of anharmonic effects, which usually are ascribed to the

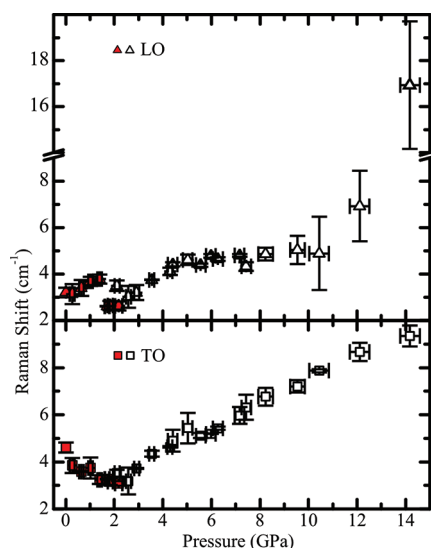


Figure 7. fwhm of the TO and LO as a function of the applied pressure. Filled and open symbols correspond to the LP and HP series, respectively.

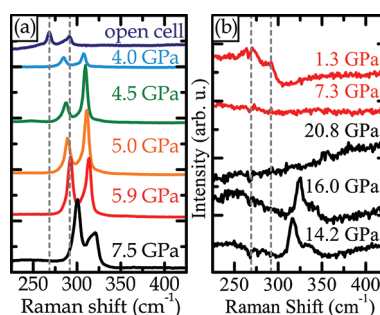


Figure 8. (a) Spectra collected at selected pressures during the depressurization phase after a maximum pressure of 11.3 GPa. (b) Spectra collected at selected pressures for increasing the pressure up to 20.8 GPa (solid black lines) and afterward decreasing the pressure (solid red lines). The gray vertical dashed lines indicate the position of the TO and LO modes in the spectrum of pristine nanowires.

decay of the phonon into two lower energy phonons. Although we have found a clear indication of electron–phonon coupling (Fröhlich interaction), it is unclear which decay mechanism is responsible for the pressure dependence of the fwhm of the TO phonon. The fwhm of the SO and 2LO modes (not plotted in the figure) stay approximately constant.

Phase Transitions. Finally, we want to comment on the behavior of the nanowires when depressurizing the cell. Two different sets of measurements were performed using two different types of cell. A third set of measurements was performed up to 11.3 GPa with the screw-clamped opposing-plate DAC with the 400 μm culet diamonds. When depressurizing the opposing-plate DAC, Raman spectra were collected at selected pressures and the resonances of the phonon intensities were observed, as shown in Figure 8a. The Raman spectrum of the nanowires pressurized up to 20.8 GPa appears clearly different from the spectrum

of pristine nanowires, as shown in Figure 8b. For $P > 16$ GPa, as well as in the down direction, the Raman spectrum does not exhibit any clear signals anymore at the highest pressure and after depressurising down to 7.3 GPa. At very low pressure some broad features reappear in the frequency range of the TO and LO modes of the pristine wires. Similar phenomena were already observed in bulk GaAs and were interpreted as an indication of a partial phase transition from GaAs zincblende to GaAs orthorhombic structure.³⁰ Further experimental investigations on nanowires are needed to clarify their behavior with respect to structural phase transitions.

CONCLUSION

In conclusion, we have performed photoluminescence and Raman scattering experiments on zincblende GaAs nanowires as a function of hydrostatic pressures up to 21 GPa. The E_0 and the $E_0 + \Delta_{SO}$ gaps have been tuned by means of applied pressure, enabling resonant Raman scattering with fixed excitation energy. The 2LO mode exhibits a sharp outgoing

resonance, which is stronger than that of the LO resonance. This is attributed to an electron–phonon Fröhlich interaction. The Grüneisen parameters of the optical modes at Γ were found to be slightly smaller than those of bulk GaAs. This is a signature of an increased covalent character of the system, in agreement with the reduced value of the effective dynamical charge at low pressure. However, the dependence of the effective dynamical charge on the relative lattice compression is relatively weak, indicating a resistance of the nanowires to become more covalent upon compression, with respect to the bulk. This may be attributed either to a modification of the ionicity of the system due to the large surface to volume ratio or to a different response of the unit cell volume to applied pressure. In our calculation, we assumed the same dependence of the lattice compression on applied pressure as for the bulk. High-pressure X-ray scattering experiments could clarify this aspect. Finally, we found a strong indication of a structural phase transition of the nanowires above 16 GPa.

METHODS

Light-scattering experiments on zinc-blende GaAs nanowires under hydrostatic pressure up to 20.8 GPa were performed by using a DAC with a 4:1 methanol–ethanol mixture as pressure-transmitting medium. Spectra were collected on disordered bundles of nanowires, mechanically deposited within the DAC. Two series of measurements were carried out: in one case, pressure was raised from ambient condition up to 2.2 GPa, in steps of ~ 0.3 GPa, using a screw-clamped opposing-plate DAC, and in the other case the pressure was raised to 20.8 GPa in much larger pressure steps using a gas-driven membrane DAC. Both the cells were equipped with 700–800 μm culet II A diamonds and molybdenum (Mo) gaskets, in which a sample chamber of 150 μm diameter was drilled. The gasket for the LPS was obtained from a 150 μm thick Mo foil, and that for the HPS from a 250 μm Mo foil, reaching a 40–50 μm thickness under working conditions. Raman and PL spectra were measured in backscattering geometry, using a micro-Raman spectrometer (Labram Infinity from Jobin Yvon) with a charge-coupled device (CCD) detector and an adjustable notch filter to reject elastically scattered light. The samples were excited by the 632.8 nm ($E_L = 1.959$ eV) line of a 20 mW He–Ne laser. Optical density filters were used in order to attenuate the power density of the laser, avoiding heating effects.^{31,32} The microscope was equipped with a 50 \times magnification objective, which gives a laser spot of about 1 μm in diameter, and the confocal diaphragm was adjusted to 50 μm . The PL signal was measured with the 600 lines/mm grating. Since the position in energy of the PL depends on the applied pressure,^{12,15} the grating was centered consequently. The 1800 lines/mm grating was used in order to measure the Raman spectra over the 200–1100 cm^{-1} frequency range. Both PL and Raman spectra were collected from two different nanowire ensembles, in order to monitor the homogeneity of the sample at each working pressure. We notice that despite the effort spent to locate the laser spot always on the same two chosen nanowire ensembles, the accuracy of the spatial positioning was experimentally limited. Raman spectra were also collected when releasing the DAC from the maximum pressure. Pressure was measured *in situ* by the ruby luminescence method³³ before and after collecting the PL and Raman spectra.

GaAs nanowires were grown by molecular beam epitaxy by the gallium-assisted method,³⁴ at 630 $^\circ\text{C}$ and at an As pressure

of 3.0×10^{-6} mbar for 2 h. These growth conditions result in GaAs nanowires that are about 9 μm long, with a diameter of about 80 nm, and with a 100% zincblende structure as discussed in detail in ref 1.

Conflict of Interest: The authors declare no competing financial interest.

Acknowledgment. We kindly thank M. Bichler and H. Riedl for excellent experimental help. This work was supported financially by the DFG via the excellence cluster Nanosystems Initiative Munich (NIM) and the SFB 631, and by the EU via the Marie Curie Excellence Grant “SENFED”. I.Z. and G.A. also thank the TUM Institute for Advanced Study for support.

REFERENCES AND NOTES

- Spirkoska, D.; Arbiol, J.; Gustafsson, A.; Conesa-Boj, S.; Glas, F.; Zardo, I.; Heigoldt, M.; Gass, M. H.; Bleloch, A. L.; Estrade, S.; *et al.* Structural and Optical Properties of High Quality Zinc-Blende/Wurtzite GaAs Nanowire Heterostructures. *Phys. Rev. B* **2009**, *80*, 245325.
- Ikonic, Z.; Srivastava, G. P.; Inkson, J. C. Electronic Properties of Twin Boundaries and Twinning Superlattices in Diamond-Type and Zinc-Blende-Type Semiconductors. *Phys. Rev. B* **1993**, *48*, 17181–17193.
- Moore, A. L.; Saha, S. K.; Prasher, R. S.; Shi, L. Phonon Backscattering and Thermal Conductivity Suppression in Sawtooth Nanowires. *Appl. Phys. Lett.* **2008**, *93*, 083112.
- Cardona, M. Effects of Pressure on the Phonon-Phonon and Electron-Phonon Interactions in Semiconductors. *Phys. Status Solidi B* **2004**, *241*, 3128–3137, and references therein.
- Zardo, I.; Conesa-Boj, S.; Peiro, F.; Morante, J. R.; Arbiol, J.; Uccelli, E.; Abstreiter, G.; Fontcuberta i Morral, A. Raman Spectroscopy of Wurtzite and Zinc-Blende GaAs Nanowires: Polarization Dependence, Selection Rules, and Strain Effects. *Phys. Rev. B* **2009**, *80*, 245324.
- Ketterer, B.; Heiss, M.; Uccelli, E.; Arbiol, J.; Fontcuberta i Morral, A. Untangling the Electronic Band Structure of Wurtzite GaAs Nanowires by Resonant Raman Spectroscopy. *ACS Nano* **2011**, *5*, 7585–7592.
- Brewster, M.; Schimek, O.; Reich, S.; Gradecak, S. Exciton-Phonon Coupling in Individual GaAs Nanowires Studied

- Using Resonant Raman Spectroscopy. *Phys. Rev. B* **2009**, *80*, 201314.
8. Moller, M.; de Lima, M. M., Jr.; Cantarero, A.; Dacal, L. C. O.; Madureira, J. R.; Iikawa, F.; Chiaramonte, T.; Cotta, M. A. Polarized and Resonant Raman Spectroscopy on Single InAs Nanowires. *Phys. Rev. B* **2011**, *84*, 085318.
 9. Khachadorian, S.; Papagelis, K.; Scheel, H.; Colli, A.; Ferrari, A. C.; Thomsen, C. High Pressure Raman Scattering of Silicon Nanowires. *Nanotechnology* **2011**, *22*, 195707.
 10. Wei, S.-H.; Zunger, A. Predicted Band-Gap Pressure Coefficients of All Diamond and Zinc-Blende Semiconductors: Chemical Trends. *Phys. Rev. B* **1999**, *60*, 5404–5411.
 11. Paul, W. The Effect of Pressure on the Properties of Germanium and Silicon. *J. Phys. Chem. Solids* **1959**, *8*, 196–204.
 12. Welber, B.; Cardona, M.; Kim, C. K.; Rodriguez, S. Dependence of the Direct Energy Gap of GaAs on Hydrostatic Pressure. *Phys. Rev. B* **1975**, *12*, 5729–5738.
 13. Goni, A. R.; Strössner, K.; Syassen, K.; Cardona, M. Pressure Dependence of Direct and Indirect Optical Absorption in GaAs. *Phys. Rev. B* **1987**, *36*, 1581–1587.
 14. Demichel, O.; Heiss, M.; Bleuse, J.; Mariette, H.; Fontcuberta i Morral, A. Impact of Surfaces on the Optical Properties of GaAs Nanowires. *Appl. Phys. Lett.* **2010**, *97*, 201907.
 15. Yu, P. Y.; Welber, B. High Pressure Photoluminescence and Resonant Raman Study of GaAs. *Solid State Commun.* **1978**, *25*, 209–211.
 16. Trommer, R.; Cardona, M. Resonant Raman Scattering in GaAs. *Phys. Rev. B* **1978**, *17*, 1865–1876.
 17. Murnaghan, F. D. The Compressibility of Media under Extreme Pressures. *Proc. Acad. Sci. U. S. A.* **1944**, *30*, 244–247.
 18. McSkimin, H. J.; Jayaraman, A.; Andreatch, P., Jr. Elastic Moduli of GaAs at Moderate Pressures and the Evaluation of Compression to 250 kbar. *J. Appl. Phys.* **1967**, *38*, 2362–2364.
 19. Shen, L. H.; Li, X. F.; Ma, Y. M.; Yang, K. F.; Lei, W. W.; Cui, Q. L.; Zou, G. T. Pressure-Induced Structural Transition in AlN Nanowires. *Appl. Phys. Lett.* **2006**, *89*, 141903.
 20. Qadri, S. B.; Yang, J.; Ratna, B. R.; Skelton, E. F. Pressure Induced Structural Transitions in Nanometer Size Particles of PbS. *Appl. Phys. Lett.* **1996**, *69*, 2205–2207.
 21. Poswal, H. K.; Garg, N.; Sharma, S. M.; Busetto, E.; Sikka, S. K.; Gundiah, G.; Deepak, F. L.; Rao, C. N. R. Pressure-Induced Structural Phase Transformations in Silicon Nanowires. *J. Nanosci. Nanotechnol.* **2005**, *5*, 729–732.
 22. dos Santos, C. L.; Piquini, P. Diameter Dependence of Mechanical, Electronic, and Structural Properties of InAs and InP Nanowires: A First-Principles Study. *Phys. Rev. B* **2010**, *81*, 075408.
 23. Trommer, R.; Müller, H.; Cardona, M.; Vogl, P. Dependence of the Phonon Spectrum of InP on Hydrostatic Pressure. *Phys. Rev. B* **1980**, *21*, 4869–4877.
 24. Goni, A. R.; Siegle, H.; Syassen, K.; Thomsen, C.; Wagner, J. M. Effect of Pressure on Optical Phonon Modes and Transverse Effective Charges in GaN and AlN. *Phys. Rev. B* **2001**, *64*, 035205.
 25. Weinstein, B. A.; Zallen, R. Pressure-Raman Effects in Covalent and Molecular Solids. In *Light Scattering in Solids IV*; Springer: Heidelberg, 1984.
 26. Trommer, R.; Anastassakis, E.; Cardona, M. In *Light Scattering in Solids*; Flammarion: Paris, 1976.
 27. Weinstein, B. A.; Renucci, J. B.; Cardona, M. Effect of Hydrostatic Pressure on the Second Order Raman Spectrum of GaP. *Solid State Commun.* **1973**, *12*, 473–479.
 28. Aoki, K.; Anastassakis, E.; Cardona, M. Dependence of Raman Frequencies and Scattering Intensities on Pressure in GaSb, InAs, and InSb Semiconductors. *Phys. Rev. B* **1984**, *30*, 681–687.
 29. Weinstein, B. A. Pressure Dependent Optical Phonon Anharmonicity in GaP. *Solid State Commun.* **1976**, *20*, 999–1003.
 30. Besson, J. M.; Itié, J. P.; Polian, A.; Weill, G.; Mansot, J. L.; Gonzales, J. High-Pressure Phase Transition and Phase Diagram of Gallium Arsenide. *Phys. Rev. B* **1991**, *44*, 4214–4234.
 31. Yazji, S.; Zardo, I.; Soini, M.; Postorino, P.; Fontcuberta i Morral, A.; Abstreiter, G. Local Modification of GaAs Nanowires Induced by Laser Heating. *Nanotechnology* **2011**, *22*, 325701.
 32. Paolone, A.; Sacchetti, A.; Corridoni, T.; Postorino, P.; Cantelli, R.; Rouse, G.; Masquelier, C. MicroRaman Spectroscopy on LiMn₂O₄: Warnings on Laser-Induced Thermal Decomposition. *Solid State Ionics* **2004**, *170*, 135–138.
 33. Mao, H.-k.; Xu, J.; Bell, P. M. Calibration of the Ruby Pressure Gauge to 800 kbar Under Quasi-Hydrostatic Conditions. *J. Geophys. Res.* **1986**, *91*, 4673–4676.
 34. Colombo, C.; Spirkoska, D.; Frimmer, M.; Abstreiter, G.; Fontcuberta i Morral, A. Ga-Assisted Catalyst-Free Growth Mechanism of GaAs Nanowires by Molecular Beam Epitaxy. *Phys. Rev. B* **2008**, *77*, 155326.